ELSEVIER

Biophysical Chemistry 78 (1999) 89–96

Biophysical Chemistry

Optimized atomic radii for protein continuum electrostatics solvation forces

Mafalda Nina, Wonpil Im, Benoît Roux*

Departments of Physics and Chemistry, Université de Montréal, C.P. 6128, succ. Centre-Ville, Montréal, QC, Canada H3C 3J7

Received 26 November 1998; received in revised form 2 December 1998; accepted 3 December 1998

Abstract

Recently, we presented a Green's function approach for the calculation of analytic continuum electrostatic solvation forces based on numerical solutions of the finite-difference Poisson–Botzmann (FDPB) equation [Im et al., Comp. Phys. Comm. 111 (1998) 59]. In this treatment the analytic forces were explicitly defined as the first derivative of the FDPB continuum electrostatic free energy with respect to the coordinates of the solute atoms. A smooth intermediate region for the solute–solvent dielectric boundary needed to be introduced to avoid abrupt discontinuous variations in the solvation free energy and forces as a function of the atomic positions. In the present paper we extend the set of optimized radii, which was previously parametrized from molecular dynamics free energy simulations of the 20 standard amino acids with explicit solvent molecules [Nina et al., J. Phys. Chem. 101 (1997) 5239], to yield accurate solvation free energy by taking the influence of the smoothed dielectric region into account.

Keywords: Analytic continuum electrostatic solvation forces; Finite-difference Poisson–Botzmann (FDPB) equation; Solute–solvent dielectric boundary; Optimized radii; Amino acids

1. Introduction

Macroscopic continuum electrostatics approaches based on numerical solutions of the finite-difference Poisson–Boltzmann (FDPB) equation are of particular interest for incorporating solvent effects implicitly in detailed atomic models of macromolecular solutes of irregular shape [1–3]. Current extension of the FDPB methodology involves the parametrization and development of computational approaches for accurately calculating the electrostatic solvation energy and forces. In this paper we review and extend our previous work on this subject [4,5].

In most practical applications, the FDPB equation is solved numerically for a fixed conformation of the solute and the free energy of solvation is calculated [1–3,5,6]. To obtain meaningful re-

* Corresponding author. Tel.: +1 514 3437105; fax: +1 514 3437586; e-mail: rouxb@plgcn.umontreal.ca

0301-4622/99/$ - see front matter
PII: S0301-4622(98)00236-1

sults, it is important to optimize the accuracy of the continuum electrostatic model for peptides and proteins. The electrostatic energy and forces depend sensitively on the nature and location of the solute–solvent dielectric boundary. This is due to the fact that the charge density caused by the solvent polarization giving rise to the solvent reaction field is concentrated at the solute–solvent dielectric boundary [5,7]. Thus, the parameterization of an accurate continuum electrostatic model requires the development of optimal sets of atomic radii for all the amino acids. Different parameterizations have been proposed to reproduce experimental and theoretical solvation free energies. For a number of small molecules, atomic radii (and charges) have been optimized from existing force fields to be in accord with experimental data; results from numerical solution of the Poisson equation have been compared to free energy simulations with explicit water molecules [6,8–13]. We have developed a set of optimized atomic radii for the 20 standard amino acids using free energy molecular dynamics simulations with explicit water molecules as a reference for the parametrization [5].

One important extension of the current FDPB methodology is to allow the calculation of solvation forces, i.e. the first derivatives of the solvation free energy with respect to the atomic coordinates of the solute. For example, the analytical forces can be used to relax the initial geometry of a flexible solute using energy minimization algorithms and make it possible to sample the conformational space using dynamical trajectories or force-biased Monte-Carlo algorithms [14,15]. Several treatments have been proposed to compute the solvation forces [16–20]. Recently, we presented a different view of the calculation of the analytical forces based on numerical solutions of the FDPB equation using a Green's function analysis [4]. A smooth intermediate region was introduced at the solute–solvent dielectric boundary to avoid abrupt discontinuous variations in the solvation free energy and forces. In this treatment the forces are explicitly equal to the first derivatives of the FDPB continuum electrostatic free energy with respect to the coordinates of the solute atoms. This insures conservation of energy and consistency of the results between dynamical and Metropolis Monte Carlo simulations. The analytical forces were shown to be equivalent to those of Gilson et al. [19,20] in the limit of an infinite grid with infinitesimal grid mesh.

The current set of optimized radii, parameterized for a continuum electrostatic model with an abrupt solute–solvent boundary, is not adequate for a model based on a smooth solute–solvent dielectric boundary region and does not provide accurate solvation free energies for the 20 standard amino acids [5]. The goal of the present paper is to determine a set of optimal radii for FDPB calculations taking into account the width of the intermediate solute–solvent dielectric boundary region. In Section 2, the methodology for calculating the electrostatic solvation forces based on the FDPB equation is reviewed. The parametrization of the atomic radii used in FDPB calculations is described in Section 3. The paper is concluded with a brief summary in Section 4.

2. Solvation forces based on the FDPB equation

We consider a molecular solute in a fixed configuration immersed in a polar solvent containing mobile ions. The conformation of the solute is described by the set of cartesian coordinates $\{\mathbf{r}_\alpha\}$. The solvation free energy of the solute in this fixed conformation may be expressed as the reversible thermodynamic work in a step-by-step process. In a first step, the neutral solute is inserted in the solvent. In a second step, the electrostatic interactions between the solute and the solvent are switched on. Thus, the solvation free energy is expressed as the sum of non-polar (np) and electrostatic (elec) contributions, $\Delta G_{\mathrm{solv}} = \Delta G_{\mathrm{np}} + \Delta G_{\mathrm{elec}}$. The non-polar contribution to the solvation free energy includes the cavity formation energy in the solvent as well as the solvent–solute van der Waals interaction energy. Traditionally, it is represented as the product of the surface of the solute and a phenomenological surface tension coefficient [19,21–23]. The electrostatic contribution to the solvation free energy is calculated on the basis of macroscopic contin-

uum electrostatics as [1–3],

$$\Delta G_{\text{elec}} = \frac{1}{2}\int \mathrm{d}\mathbf{r}\ \phi_{rf}(\mathbf{r})\rho(\mathbf{r}) \tag{1}$$

where the electrostatic solvent reaction field $\phi_{rf}(\mathbf{r})$ corresponds to the difference between the electrostatic potential computed in vacuum [$\phi(\mathbf{r}$; vacuum)] and the electrostatic potential computed with the solvent medium [$\phi(\mathbf{r}$; solvent)]. In both case, the electrostatic potential $\phi(\mathbf{r})$ is calculated by solving the linear Poisson–Boltzmann (PB) equation [1–3],

$$\nabla\cdot[\epsilon(\mathbf{r})\nabla\phi(\mathbf{r})] - \bar{\kappa}^2(\mathbf{r})\phi(\mathbf{r}) = -4\pi\rho(\mathbf{r}) \tag{2}$$

where $\epsilon(\mathbf{r})$, $\bar{\kappa}(\mathbf{r})$, and $\rho(\mathbf{r})$ are the dielectric constant, the modified Debye–Hückel screening factor, and the fixed charge density of the solute, respectively. In the solvent environment, the dielectric constant and the modified Debye–Hückel screening factor at a point, $\mathbf{r}$, are defined as a function of the position of all the atoms, $\{\mathbf{r}_\alpha\}$, in the system,

$$\epsilon(\mathbf{r}) = 1 + (\epsilon_s - 1)H(\mathbf{r};\{\mathbf{r}_\alpha\}) \tag{3}$$

and

$$\bar{\kappa}^2(\mathbf{r}) = \bar{\kappa}_b^2 H(\mathbf{r};\{\mathbf{r}_\alpha\}) \tag{4}$$

where ϵ_s is the dielectric constant of the solvent, $\bar{\kappa}^2 = 8\pi I/k_{\text{B}}T\epsilon_s$ is the screening factor of the electrolyte bulk solvent, I is the ionic strength, and $H(\mathbf{r})$ is a volume exclusion function. The electrostatic potential computed in vacuum is obtained by setting the dielectric constant and the modified Debye–Hückel screening factor to 1 and 0, respectively, at all points in space. There are several approaches to construct the volume exclusion function $H(\mathbf{r};\{\mathbf{r}_\alpha\})$ used in Eqs. (3) and (4) (see the discussion in [5]). According to an analysis based on statistical mechanical integral equation theories the excluded volume function is equal to one in the solvent region and zero in the interior of the solute to lowest order in the solvent structure [24].

In the present work, we assume that the excluded volume function is constructed on the basis of overlapping spherically-symmetric exclusion atomic spheres [5]

$$H(\mathbf{r};\{\mathbf{r}_\alpha\}) = \prod_\alpha H_\alpha(|\mathbf{r}-\mathbf{r}_\alpha|) \tag{5}$$

In finite-difference (FD) calculations, the PB equation is expressed as [1,2]

$$\begin{aligned}
&\epsilon_x(i,j,k)[\phi(i+1,j,k)-\phi(i,j,k)]\\
&\quad+\epsilon_x(i-1,j,k)[\phi(i-1,j,k)-\phi(i,j,k)]\\
&\quad+\epsilon_y(i,j,k)[\phi(i,j+1,k)-\phi(i,j,k)]\\
&\quad+\epsilon_y(i,j-1,k)[\phi(i,j-1,k)-\phi(i,j,k)]\\
&\quad+\epsilon_z(i,j,k)[\phi(i,j,k+1)-\phi(i,j,k)]\\
&\quad+\epsilon_z(i,j,k-1)[\phi(i,j,k-1)-\phi(i,j,k)]\\
&\qquad-\bar{\kappa}^2(i,j,k)\phi(i,j,k)h^2 = -4\pi\frac{q(i,j,k)}{h}
\end{aligned} \tag{6}$$

where h is the grid spacing, $\phi(i,j,k)$ is the electrostatic potential, $\bar{\kappa}(i,j,k)$ is the modified Debye–Hückel screening factor, and $q(i,j,k)$ is the fractional charge at the grid point (x_i,y_j,z_k). The fractional charge is related to the density at the grid points through $\rho(i,j,k) = q(i,j,k)/h^3$. The arrays $\epsilon_x(i,j,k)$, $\epsilon_y(i,j,k)$, and $\epsilon_z(i,j,k)$ represent the dielectric constants associated with the x-, y-, and z-directions grid branches $(x_i+h/2,y_j,z_k)$, $(x_i,y_j+h/2,z_k)$, and $(x_i,y_j,z_k+h/2)$ originating at the grid point (x_i,y_j,z_k). The FDPB equation may be conveniently expressed as a matrix algebra problem,

$$\mathbf{M}\cdot\vec{\phi} = -4\pi\vec{q} \tag{7}$$

where $\mathbf{M}$ is a symmetric matrix, and $\vec{\phi}$ and $\vec{q}$ are column vectors associated with the electrostatic potentials and the fractional charges, respectively, whose number of elements is equal to the number of grid points. The formal solution to Eq. (7) is expressed as

$$\vec{\phi} = -4\pi\mathbf{M}^{-1}\cdot\vec{q} \tag{8}$$

The inverse matrix $\mathbf{M}^{-1}$ corresponds to the formal Green's function to the FDPB equation.

According to Eqs. (1) and (8), the electrostatic contribution to the solvation free energy is given by

$$\Delta G_{\text{elec}} = \frac{1}{2}\left(\vec{\phi}_s^t - \vec{\phi}_v^t\right)\cdot\vec{q} = \frac{1}{2}(-4\pi\vec{q}^t)\cdot(\mathbf{M}_s^{-1} - \mathbf{M}_v^{-1})\cdot\vec{q} \quad (9)$$

where the superscript 't' indicates the transposed associated vector (v, vacuum; s, solvent). The analytical 'electrostatic solvation forces' correspond to the first derivatives of ΔG_{elec} with respect to the atomic coordinates of the solute. It should be noted that both the $\mathbf{M}$ matrix and the charge vector $\vec{q}$ are functions of the atomic positions $\{\mathbf{r}_\alpha\}$ of the solute due to the spatial-dependence of the dielectric function $\epsilon(\mathbf{r};\{\mathbf{r}_\alpha\})$ and Debye–Hückel screening factor $\kappa(\mathbf{r};\{\mathbf{r}_\alpha\})$. The solvation forces are given by [4],

$$\begin{aligned}\mathbf{F}_\alpha^{\text{elec}} &= -\frac{\partial\Delta G_{\text{elec}}}{\partial\mathbf{r}_\alpha}\\ &= 2\pi\frac{\partial}{\partial\mathbf{r}_\alpha}\left[\vec{q}^t\cdot(\mathbf{M}_s^{-1} - \mathbf{M}_v^{-1})\cdot\vec{q}\right]\\ &= 2\pi\left[2\vec{q}^t\cdot(\mathbf{M}_s^{-1} - \mathbf{M}_v^{-1})\cdot\frac{\partial\vec{q}}{\partial\mathbf{r}_\alpha}\right.\\ &\quad\left. -\vec{q}^t\cdot\mathbf{M}_s^{-1}\cdot\frac{\partial\mathbf{M}_s}{\partial\mathbf{r}_\alpha}\cdot\mathbf{M}_s^{-1}\cdot\vec{q}\right] \quad (10)\end{aligned}$$

where $\partial\mathbf{M}_v^{-1}/\partial\mathbf{r}_\alpha = 0$ since the dielectric constant function of the reference vacuum system is uniform through all space ($\epsilon_v = 1$). The explicit inverse $\mathbf{M}^{-1}$ in Eq. (10) may be avoided by using the formal solution Eq. (8) [4].

In the continuum limit, the first derivative may also be written as,

$$\mathbf{F}_\alpha^{\text{elec}} = -\int_V \mathrm{d}^3\mathbf{r}\left[(\phi_s - \phi_v)\frac{\partial\rho}{\partial\mathbf{r}_\alpha} + \frac{1}{8\pi}\phi_s\nabla\times\left(\frac{\partial\epsilon}{\partial\mathbf{r}_\alpha}\nabla\phi_s\right) - \frac{1}{8\pi}\phi_s^2\frac{\partial\bar{\kappa}^2}{\partial\mathbf{r}_\alpha}\right] \quad (11)$$

Contributions involving terms such as $\partial\epsilon(\mathbf{r};\{\mathbf{r}_\gamma\})/\partial\mathbf{r}_\alpha$ yield discontinuous variations of the electrostatic solvation forces if the dielectric function is constructed as a sharp Heaviside step-function. To obtain accurate estimates of the solvation forces, an intermediate dielectric region is introduced at the solute–solvent boundary. For the sake of convenience, the transition region of the excluded volume function is constructed as a simple polynomial,

$$H_\alpha(r) = \begin{cases} 0, & r \le R_\alpha - w \\ -\frac{1}{4w^3}(r - R_\alpha + w)^3 + \frac{3}{4w^2}(r - R_\alpha + w)^2, & R_\alpha - w < r < R_\alpha + w \\ 1, & r \ge R_\alpha + w \end{cases} \quad (12)$$

where r is the distance between a point on the system and atom α, R_α is the radius of atom α, and w is the half-width of the transition region. The calculation of analytic derivatives of the electrostatic solvation free energy was implemented in the PBEQ module (Beglov et al., unpublished) in the CHARMM biomolecular simulation program [25].

3. Parametrization of atomic radii

It is important to optimize the accuracy of the continuum electrostatic model used to compute the electrostatic solvation free energy and forces. In a previous paper [5], we proposed to achieve this by using molecular dynamics simulations of an all-atom molecular mechanics model with explicit water molecules as the reference. This choice was motivated in part by the difficulty in obtaining reliable measurements of the absolute excess solvation free energy for the 20 standard amino acids in water. Furthermore, experimental solvation free energies cannot be easily separated into cavity and electrostatic contributions. One additional advantage of choosing this approach is its consistency. Properties calculated with the

continuum model with optimized radii are determined by what is the best currently available microscopic model of solvation. The ability to compare both microscopic and macroscopic models provides a sound basis to apply macroscopic approaches to a wide range of biological problems.

The solvation free energies of the amino acids were computed using a modified version of the PERT facility of CHARMM [25], following standard free energy perturbation techniques [26,27]. The non-zwitterionic tripeptide (*N*)-acetyl-X-(*N′*)-methylamide (CH_3–CO–NH–CR–CO–NH–CH_3), was chosen as a model of the protein backbone, where X is Gly, Ala, Val, Ile, Leu, Phe, Tyr, Cys, Trp, Arg, Glu, Asp, Lys, Thr, Pro, Met, Ser, His, Asn and Gln (R is the corresponding side chain). Asp and Glu side chains were deprotonated, His is neutral (protonated on ND1) and Lys and Arg were protonated. The all-hydrogen PARM22 potential function of CHARMM [28] was used. Each tripeptide was hydrated in a sphere of 150 TIP3P water molecules [29]. A spherical solvent boundary potential (SSBP) was used to approximate the influence of the surrounding bulk water [30]. The free energy of charging a molecule was calculated for each individual amino acid using 10 windows with the scaled charges of the tripeptide $\lambda \times q_i$. The configurational sampling was performed using 15 ps of Langevin dynamics for each window, varying λ_i from 0.05 to 0.95 ± 0.10 by an increment of 0.10. The electrostatic solvation free energy differences were combined using the weighted histogram analysis method (WHAM) [31].

The results of the free energy molecular dynamics calculations are given in Table 1 (MD). A set of atomic Born radii for proteins R_α was optimized, on the basis of the average radial solvent charge distribution functions, to quantitatively reproduce the results from the free energy simulations with explicit water molecules [5]. The optimization was based on the standard FDPB model with an abrupt solute–solvent dielectric

Table 1
Electrostatic free energy contribution (in kcal/mol) for the 20 standard amino acids[a]

Residue	Smoothing window *w* (in Å)									MD	*w* = 0
	0.2	0.3	0.4	0.5	0.6	0.7	0.8	0.9	1.0		
Gly	−13.3	−13.3	−13.3	−13.3	−13.4	−13.4	−13.4	−13.3	−13.2	−13.3	−13.2
Ala	−12.1	−12.1	−12.0	−12.0	−11.9	−11.8	−11.6	−11.5	−11.3	−11.9	−12.0
Val	−10.6	−10.5	−10.4	−10.3	−10.2	−10.1	−10.0	−9.7	−9.6	−10.4	−10.5
Leu	−11.9	−11.8	−11.8	−11.7	−11.6	−11.4	−11.3	−11.0	−10.8	−11.4	−11.8
Ile	−10.5	−10.6	−10.4	−10.2	−10.1	−10.0	−9.8	−9.6	−9.5	−10.8	−10.4
Pro	−16.5	−16.4	−16.3	−16.2	−16.1	−16.0	−15.8	−15.6	−15.4	−16.5	−16.4
Cys	−15.5	−15.5	−15.4	−15.3	−15.2	−15.1	−14.9	−14.8	−14.6	−15.5	−15.4
Met	−11.2	−11.2	−11.1	−11.1	−11.0	−10.9	−10.8	−10.6	−10.4	−11.2	−11.1
Thr	−18.1	−18.0	−17.7	−17.5	−17.3	−17.0	−16.7	−16.4	−16.1	−18.1	−17.9
Ser	−19.7	−19.6	−19.5	−19.4	−19.2	−19.2	−19.1	−19.0	−18.8	−19.7	−19.6
Phe	−15.3	−15.1	−14.8	−14.6	−14.3	−14.0	−13.6	−13.2	−12.8	−14.6	−14.7
Trp	−17.8	−17.6	−17.3	−17.0	−16.7	−16.4	−16.0	−15.6	−15.2	−17.9	−17.8
Tyr	−19.8	−19.7	−19.6	−19.4	−19.2	−19.0	−18.7	−18.4	−18.2	−19.0	−19.1
Asn	−20.9	−20.9	−20.9	−20.8	−20.8	−20.7	−20.5	−20.3	−20.1	−20.8	−20.8
Gln	−16.7	−16.7	−16.7	−16.7	−16.6	−16.5	−16.4	−16.3	−16.2	−16.7	−16.6
Asp	−90.8	−90.4	−90.0	−89.5	−89.0	−88.5	−87.8	−87.2	−86.5	−91.9	−91.0
Glu	−88.0	−87.6	−87.1	−86.7	−86.1	−85.6	−84.9	−84.3	−83.5	−87.8	−88.3
His	−26.0	−26.0	−26.0	−25.9	−25.7	−25.5	−25.2	−24.8	−24.4	−25.7	−25.9
Lys	−73.6	−73.7	−73.8	−73.8	−73.8	−73.8	−73.8	−73.9	−73.9	−72.9	−72.9
Arg	−67.0	−67.0	−67.0	−66.8	−66.8	−66.6	−66.6	−66.4	−66.3	−66.0	−66.3

[a]All FDPB calculations were performed with a grid of 100 points and a spacing of 0.2 Å with no ionic strength using the PBEQ module (Im et al., unpublished) of the CHARMM program [25].

boundary ($w = 0$). All hydrogen atoms were assigned a radius of 0 Å in the optimized set. As can be seen in Table 1, the optimized atomic radii yield accurate free energies that are in excellent agreement with the results from molecular dynamics simulations (given in columns $w = 0$ and MD, respectively).

The width of the dielectric transition region in Eq. (12) has an important influence on the magnitude of the calculated electrostatic free energy of solvation. For this reason, the previous set of radii is not optimal when a finite dielectric transition region of width $2w$ is introduced. This effect may be illustrated by considering simple dielectric models for a spherical ion. Fig. 1 shows various models for the excluded volume function around a spherical ion of 2-Å radius. The simplest model, corresponding to case (a) in Fig. 1, assumes that the dielectric constant changes abruptly from 1 to 80. The electrostatic solvation free energy calculated with Eqs. (6),(1) is -82.85 kcal/mol [the FDPB equation was solved using a cubic grid of $(43)^3$ points with a spacing of 0.2 Å]. The calculated value compares well with the Born model of solvation [32],

$$\Delta G_{\text{elec}} = \frac{Q^2}{2R_{\text{ion}}}\left(\frac{1}{\epsilon_s} - 1\right) \tag{13}$$

which yields a value of -82 kcal/mol for a radius of 2 Å. The difference is due to the discreteness of the grid. There are several ways to implement a dielectric transition region for a spherical ion of 2.0-Å radius, varying smoothly from 1 (in the interior of the solute) to ϵ_s, the dielectric constant of the bulk solvent. One possibility is to center the transition region on the initial radius. This is illustrated as case (b) in Fig. 1, where a dielectric region of 1.0 Å is constructed to extend from 1.5 to 2.5 Å ($w = 0.5$ Å). Solving the FDPB equation for this dielectric model using the same approach, the calculated electrostatic solvation free energy is -103.11 kcal/mol. The value is clearly overestimated compared to the initial model. A second possibility is to set the smooth dielectric region from 2.0 to 3.0 Å, at the limit of the initial radius. This is illustrated as case (d) in Fig. 1. The calculated electrostatic solvation free energy obtained from the FDPB equation is

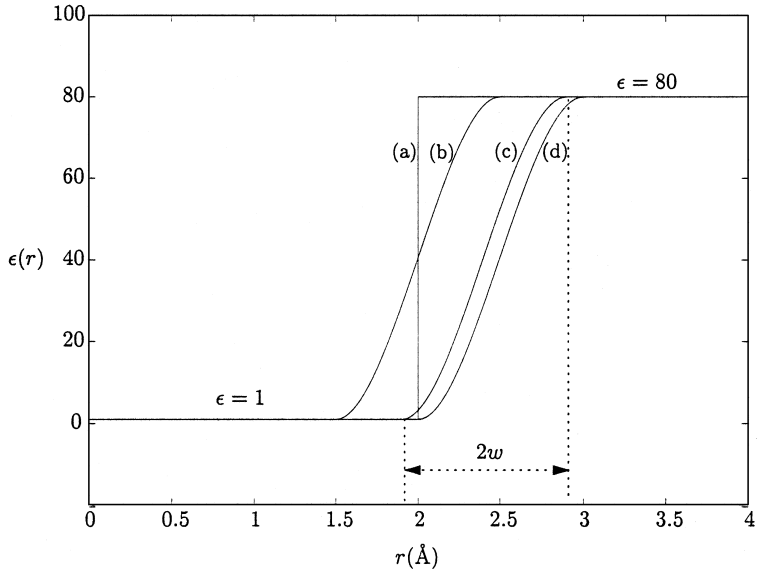

Fig. 1. Illustration of the smoothed dielectric boundary region for a single spherical ion of 2-Å radius. For a smoothing region of 0.5 Å, the free energy of the Born model with an abrupt dielectric region (a) is reproduced with a radius of 2.4 Å (c). The electrostatic solvation free energy is not well-reproduced with a smoothing region centered on the abrupt radius (case b), nor with the smoothing region outlying at the edge of the abrupt radius (case d).

−78.47 kcal/mol, almost in much better agreement with the initial solvation free energy. The result can be further improved by moving the transition region inward by 0.1 Å, which is shown as case (c) in Fig. 1. With this model, the solvation free energy calculated by solving the FDPB equation is −82.37 kcal/mol, almost in perfect agreement with model (a). The dependence of the solvation free energy upon the width of the boundary region can be better understood by considering the average reaction field solvent charge distribution around the solute [5],

$$\langle \rho_{\mathrm{elec}}(\mathbf{r})\rangle = -\nabla\cdot\left(\frac{\epsilon(\mathbf{r})-1}{4\pi}\mathbf{E}\right) \qquad (14)$$

In case (a), a sharply peaked charge distribution is localized at the solute–solvent interface (at 2.0 Å). Introducing a transition dielectric region spreads the solvent-induced reaction field charge over the width of the smoothing function. Since the electrostatic solvation free energy corresponds to the interaction between the atomic charge and the solvent-induced charge distribution, the location of the solvent charge is determinant. The best agreement with case (a) is obtained when the transition region goes from 1.9 to 2.9 Å.

The analysis suggests that a simple transformation of the radius of a spherical ion is sufficient to roughly recover the Born solvation free energy: $R_\alpha \rightarrow R_\alpha + w - 0.1$, where $w = 0.5$ is the half-width of the smoothing window. However, it may be expected that a transition region of different width should require a different adjustment to reproduce the correct electrostatic free energy. In the case of complex molecular solutes such as amino acids, the adjustment of the atomic radii must be accomplished empirically to obtain accurate electrostatic solvation free energies. In practice we found that accurate free energies were obtained using the empirical rule, $R'_\alpha = a(R_\alpha + w)$, where a is a scaling factor with a value close to 1. Values of the scaling factors with associated half-width of the smoothing window w are given in Table 2. The electrostatic solvation free energies for the 20 standard amino acids were calculated with the continuum model of solvation including an intermediate region for the solute–solvent boundary. A series of widths for the smoothing region were considered where the dielectric boundary was determined following the simple empirical rule to adjust the Born radii for all atoms (except hydrogens which have a radius of 0 Å). The results given in Table 1 indicate a very good agreement between the electrostatic solvation free energies from molecular dynamics with explicit solvent (column MD) and previous free energies from a continuum solvent model without an intermediate region for the solute–solvent boundary (column $w = 0$). The largest deviation is observed for Asp and Glu in the case of W = 1.0 Å and is on the order of 5%. For a W = 0.5 Å, or less all the electrostatic free energies deviate by at most 1%.

4. Summary

In a previous paper, we developed a rigorous formulation for the calculation of electrostatic solvation forces from a linearized Poisson–Boltzmann (PB) equation [Im et al., Comp. Phys. Comm. 111 (1998) 59]. The introduction of a smooth solute–solvent boundary was required for the computation of electrostatic forces from a continuum solvation model. In this paper, we optimized a set of atomic radii for the 20 standard amino acids for the purpose of defining a smooth dielectric boundary. A good agreement with the electrostatic contribution to the solvation free energies calculated by free energy simulation techniques with explicit water molecules was ob-

Table 2
Smoothing region and corresponding scaling factors for atomic radii[a]

w (Å)	0.1	0.2	0.3	0.4	0.5	0.6	0.7	0.8	0.9	1.0
a	0.979	0.965	0.952	0.939	0.927	0.914	0.901	0.888	0.875	0.861

[a] The modified atomic radius, $R'_\alpha = a(R_\alpha + w)$, where R_α is the original optimized atomic radius from Nina et al. [5], w is the half-width of the smoothing region (Note: the values were generated with the equation $a = -0.13w + 0.99$).

tained with this model. It was shown that the value of the solvation free energy depends both on the atomic radii and on the width of the smoothing window. An empirical adjustment of the atomic radii for the standard amino acids was found that reproduces accurately the free energies using the rule $R'_\alpha = a(R_\alpha + w)$, where a is a scaling factor close to 1, R_α is the original optimized atomic radius from [5] and w is the half-width of the smoothing window. The current set of optimized radii allows the calculation of the first derivative of the solvation free energy obtained from FDPB that is consistent with numerically-calculated solvation forces. In practical applications, the computation of the forces associated with a continuum electrostatics description of the solvent accounts for the important conformational flexibility of the solute. Furthermore, the introduction of a smooth dielectric boundary may be helpful for improving the efficiency of the FDPB calculation using multigrid methods. Those methods perform better when the coefficient of the FDBP vary continuously with the coarseness of the grid, whereas sharp dielectric discontinuities give rise to a poor convergence rate [33]. Nonetheless, the application of continuum electrostatics in molecular dynamics simulations of proteins and biomolecules is still restricted since there is poor quantitative agreement with experimental values. Future development for improving the description of total solvation free energies of the amino acids will involve the treatment of the non-polar contribution and the influence of a smooth transition region within a continuum model of solvation.

References

[1] J. Warwicker, H.C. Watson, J. Mol. Biol. 157 (1982) 671.
[2] I. Klapper, R. Hagstrom, R. Fine, K. Sharp, B. Honig, Proteins 1 (1986) 47.
[3] K.A. Sharp, B. Honig, Annu. Rev. Biophys. Biophys. Chem. 19 (1990) 301.
[4] W. Im, D. Beglov, B. Roux, Comp. Phys. Commun. 111 (1998) 59–75.
[5] M. Nina, D. Beglov, B. Roux, J. Phys. Chem. 101 (1997) 5239.
[6] A. Jean-Charles, A. Nicholls, K. Sharp, et al., J. Am. Chem. Soc. 113 (1991) 1454.
[7] R.J. Zauhar, R.S. Morgan, J. Mol. Biol. 186 (1985) 815.
[8] D. Sitkoff, K.A. Sharp, B. Honig, J. Phys. Chem. 98 (1994) 1978.
[9] C. Lim, D. Bashford, M. Karplus, J. Phys. Chem. 95 (1991) 5610.
[10] W.L. Jorgensen, J. Tirado-Rives, J. Am. Chem. Soc. 110 (1988) 1657.
[11] S.J. Weiner, P.A. Kollman, U.C. Case, et al., J. Am. Chem. Soc. 106 (1973) 765.
[12] T.J.A. Ewing, T.P. Lybrand, J. Phys. Chem. 98 (1994) 1748.
[13] T.J. Marrone, M.K. Gilson, J.A. McCammon, J. Phys. Chem. 100 (1996) 1439.
[14] M.P. Allen, D.J. Tildesley, Clarendon Press, Oxford, 1989.
[15] J.L. Smart, T.J. Marrone, J.A. McCammon, J. Comput. Chem. 18 (1997) 1750.
[16] M.E. Davis, J.A. McCammon, J. Comput. Chem. 11 (1990) 401.
[17] K. Sharp, J. Comp. Chem. 12 (1991) 454.
[18] C. Niedermeier, K. Schulten, Mol. Simulation 8 (1992) 361.
[19] M.K. Gilson, M.E. Davis, B.A. Luty, J.A. McCammon, J. Phys. Chem. 97 (1993) 3591.
[20] M.K. Gilson, J.A. McCammon, J.D. Madura, J. Comp. Chem. 16 (1995) 1081.
[21] R.B. Hermann, J. Phys. Chem. 76 (1971) 2754.
[22] K.A. Sharp, A. Nicholls, R. Friedman, B. Honig, Biochemistry 30 (1991) 9686.
[23] T. Simonson, A. Brunger, J. Phys. Chem. 98 (1994) 4683.
[24] D. Beglov, B. Roux, J. Chem. Phys. 104 (1996) 8678.
[25] B.R. Brooks, R.E. Bruccoleri, B.D. Olafson, D.J. States, S. Swaminathan, M. Karplus, J. Comp. Chem., 4 (1983) 187.
[26] T.P. Straatsma, H.J.C. Berendsen, J.P.M. Postma, J. Chem. Phys. 85 (1986) 6720.
[27] T.P. Straatsma, H.J.C. Berendsen, J.P.M. Postma, J. Chem. Phys. 89 (1988) 5876.
[28] A.D. Mackerell, Jr., D. Bashford, M. Bellot, et al., Biophys. J. 61 (1992) A143.
[29] W.L. Jorgensen, J. Chandrasekhar, J.D. Madura, R.W. Impey, M.L. Klein, J. Chem. Phys. 79 (1983) 926.
[30] D. Beglov, B. Roux, J. Chem. Phys. 100 (1994) 9050.
[31] S. Kumar, D. Bouzida, R.H. Swendsen, P.A. Kollman, J.M. Rosenberg, J. Comp. Chem. 13 (1992) 1011.
[32] M. Born, Z. Phys. 1 (1920) 45.
[33] M. Holst, F. Saied, J. Comput. Chem. 14 (1993) 105–113.